Available online at www.sciencedirect.com
ScienceDirect
Catalysis Today 120 (2007) 324–329
CATALYSIS TODAY
www.elsevier.com/locate/cattod

A porous mixed-valent iron MOF exhibiting the acs net: Synthesis, characterization and sorption behavior of $Fe_3O(F_4BDC)_3(H_2O)_3\cdot(DMF)_{3.5}$

Ji Hye Yoon [a], Sang Beom Choi [a], You Jin Oh [a], Min Jeong Seo [a], Young Ho Jhon [a], Tae-Bum Lee [b], Daejin Kim [b], Seung Hoon Choi [b], Jaheon Kim [a,*]

[a] *Department of Chemistry, Soongsil University, Seoul 156-743, Republic of Korea*
[b] *Insilicotech Co. Ltd., Seongnam-Shi 463-943, Republic of Korea*

Available online 24 October 2006

Abstract

A new mixed-valent iron MOF, formulated as $Fe_3O(F_4BDC)_3(H_2O)_3\cdot(DMF)_{3.5}$ (**1**), has been synthesized by using a perfluorinated linear dicarboxylate to link trigonal prismatic $Fe_3(\mu^3\text{-}O)(O_2C\text{–})_6$ clusters. The structure refinement based on single crystal X-ray diffraction data collected from **1** reveals the material exhibits the *acs* topology with large channels along the crystallographic *c*-axis. Due to the presence of fluorine atoms the organic link, 2,3,5,6-tetrafluorobenzene-1,4-dicarboxylate (F_4BDC), has a 63° torsion angle between the carboxylate and aromatic planes, resulting in larger channels compared to those in the isoreticular material MOF-235. While few iron-based MOFs have demonstrated porosity, nitrogen and hydrogen sorption experiments carried out at 77 K proved the porosity of outgassed **1**, which has a Langmuir surface are of 635 m^2/g and a gravimetric capacity of 0.9 wt% of hydrogen at 1 bar.

Keywords: Metal-organic framework; Hydrogen storage; Sorption; Iron; Microporous

1. Introduction

Although research remains active in the search for a practical hydrogen storage technology, systems that meet the US Department of Energy targets remain elusive [1]. The most developed systems are still high pressure tanks, operating at pressures up to 825 bar [2], however, both safety and storage efficiency issues have limited their widespread use and continue to drive the chemical research of hydrogen sorption materials.

Recently, it was reported that a series of isoreticular metal-organic frameworks (MOFs) adsorb and release hydrogen reversibly and the adsorbed quantities were dependent on the identity of the material [3]. MOFs are crystalline hybrid materials composed of metal ions or clusters that are bridged by organic ligands. A diversity of organic and inorganic building blocks has been identified to assemble their periodic frameworks [4]. Synthetic procedures usually involve simple, one-pot solvothermal reactions, with products obtained as high-purity crystalline solids. Aside from possible applications as magnetic materials due to the presence of paramagnetic metal centers, they might also function as molecular sieves, optoelectronic materials, sensors, catalysts, and storage materials [5]. This wide range of potential utility arises from the many possibilities in augmenting their framework topologies, pore dimensions, and pore environments.

Since the initial report of hydrogen adsorption in MOFs, several materials have been reported that adsorb up to ~2.5 wt% at 77 K and 1 bar [6,7]. The structural features that appear to most strongly influence the amount of uptake include the chemical composition and geometry of the inorganic clusters, and the size and shape of the pores. Recently, we suggested that the control of the electronic properties endowed to the frameworks could be another factor for consideration in designing MOFs with improved H_2 interaction energies [8]. The most important determinant of the total uptake by a material, however, is the magnitude of the pore volume.

The interpretation and prediction of MOF structures are largely dependent on the geometry of the coordinated metal clusters, referred to as secondary building units (SBUs). If the SBUs are considered as the ‘‘joints’’ and the organic links as the

* Corresponding author. Tel.: +82 2 820 0459; fax: +82 2 824 4383.
E-mail address: jaheon@ssu.ac.kr (J. Kim).

0920-5861/$ – see front matter © 2006 Elsevier B.V. All rights reserved.
doi:10.1016/j.cattod.2006.09.003

"struts" of the frameworks, the simplest and most widely observed net describing the connectivity of the material is the *default net* [9]. A typical example is MOF-5 (also known as IRMOF-1), in which the SBUs are structurally analogous to the basic zinc oxo acetate cluster [10]. These octahedral SBUs are linked by phenylene units to produce a primitive cubic net, the predicted default net. Functionalization and extension of the linear links yields structures based on the same net, allowing a degree of chemical tailoring to be accomplished [11].

While many MOFs are known that exhibit the default nets expected for the assembly of tetrahedral, square, triangular, and octahedral building blocks [9], MOF structures based on the assembly of trigonal prismatic SBUs are less common, but have attracted considerable attention [12–15]. Examples include MOF-235 and MOF-236, which were synthesized from trigonal prismatic iron oxo acetate SBUs and linear (benzene-1,4-dicarboxylate) or bent (benzene-1,3-dicarboxylate) links, respectively. The topologies of these frameworks have been analyzed and identified as the default *acs* net [16]. The materials, however, are non-porous; MOF-235 is a cationic framework with pores filled by counter anions, and the efficient packing of the neutral MOF-236 framework leaves no available room for gas storage.

In this report, we describe the preparation of a new MOF with the *acs* topology and sufficiently large pores for the sorption of nitrogen and hydrogen molecules.

2. Experimental

2.1. Physical measurements

Elemental analyses were carried out on a EA 1110, CE instrument. Thermogravimetric analyses (TGA) were performed using a Scinco TGA S-1000 instrument with a nitrogen atmosphere. IR spectra were recorded on a JASCO FT-IR-4000 spectrophotometer with samples prepared as KBr pellets. X-ray powder diffraction (XRPD) data were collected on a Rigaku MiniFlex diffractometer with Cu Kα radiation. Gas sorption measurements were carried out in the volumetric home-built apparatus at 77 K (described further below). Single crystal X-ray diffraction data were collected using a Bruker SMART CCD diffractometer.

2.2. Synthesis of $Fe_3O(F_4BDC)_3(H_2O)_3\cdot(DMF)_{3.5}$ (1)

Brown rod-shaped crystals of **1** were grown by diffusing triethylamine vapor into a solution of 2,3,5,6-tetrafluorobenzene-1,4-dicarboxylic acid (H_2F_4BDC) (0.03 g, 0.13 mmol) and $FeCl_2\cdot 4H_2O$ (0.15 g, 0.38 mmol) in a mixture of solvents *N*,*N*-dimethylformamide (DMF) (1.0 mL) and water (0.50 mL). Crystals were filtered and washed with neat DMF (3 × 5 mL) and hexanes (3 × 5 mL). The calculated yield of the air-dried sample was 64% based on stoichiometry of the organic dicarboxylic acid. The crystals are slightly soluble in water, but stable in organic solvents such as DMF, MeOH, EtOH, acetone, and DMSO. The empirical formula was determined by elemental analyses, thermogravimetric analysis (TGA) and X-ray crystallography. Anal. Calcd (%) for $Fe_3O(F_4BDC)_3(H_2O)_3\cdot(DMF)_{3.5}$: C, 34.48; H, 2.56; N, 4.08. Found: C, 34.81; H, 2.10; N, 3.84. FT-IR (KBr pellet, 4000–400 cm^{-1}): 3440 (br), 2925 (m), 2854 (w), 1641 (s), 1471 (m), 1392 (s), 1263 (w), 995 (m), 732 (m), 671 (w), 495 (w).

2.3. X-ray crystallography

A brown rod-shaped single crystal (0.38 mm × 0.10 mm × 0.10 mm) of **1** was mounted in a cryo-loop and positioned in the center of liquid nitrogen exhaust stream. X-ray data were collected using graphite monochromated Mo Kα radiation (λ = 0.71073 Å) on a Bruker SMART CCD diffractometer. A total of 5895 reflections were collected in the range $1.49^\circ < \theta < 21.11^\circ$ of which 743 were independent and 528 were observed ($I > 2\sigma(I)$). After the data integration (SAINT) and semi-empirical absorption correction based on equivalent reflections (SADABS), the structure was solved by direct methods and subsequent difference Fourier techniques (SHELX-TL). The F_4BDC was disordered over two sites with equivalent occupancies. Due to the high symmetry of the structure the solvent molecules in the pore could not be located. Application of the SQUEEZE routine in the PLATON software package produced a new intensity data set excluding the intensity contribution from disordered solvent molecules. All framework atoms were refined anisotropically and the final full-matrix least-squares refinement was converged to give $R_1 = 0.1064$ and $wR_2 = 0.2792$ ($I > 2\sigma(I)$). Crystallographic and structure refinement parameters are summarized in Table 1. Selected bond distances and angles are presented in Table 2. The crystallographic CIF

Table 1
Crystal data and structure refinement for **1**

Empirical formula	$C_{34.5}H_{30.5}N_{3.5}O_{19.5}F_{12}Fe_3$
Formula weight	1201.67
Temperature	253(2) K
Wavelength	0.71073 Å
Crystal system	Hexagonal
Space group	$P6_3/mmc$ (No. 194)
Unit cell dimensions	$a = b = 15.790(2)$ Å $c = 16.050(2)$ Å.
Volume	3465.5(8) $Å^3$
Z	2
Density (calculated)	1.152 g/cm^3
Absorption coefficient	0.704 mm^{-1}
$F(000)$	1208
Index ranges	$-15 \le h \le 15$, $-16 \le k \le 10$, $-15 \le l \le 15$
Reflections collected	5895
Independent reflections	743 [R (int) = 0.2362]
Completeness to θ	21.11°, 98.4%
Maximum and minimum transmission	0.9329 and 0.7756
Refinement method	Full-matrix least-squares on F^2
Data/restraints/parameters	743/0/58
Goodness-of-fit on F^2	1.044
Final R indices [$I > 2\sigma(I)$]	$R_1 = 0.1064$, $wR_2 = 0.2792$
R indices (all data)	$R_1 = 0.1253$, $wR_2 = 0.2907$
Largest diff. peak and hole	0.974 and −0.963 e $Å^{-3}$

Table 2
Selected bond lengths [Å] and angles [°] for **1**

Fe(1)–O(1)	1.885(2)
Fe(1)–O(3)	2.154(13)
F(2)–C(4)	1.35(2)
C(1)–O(2)[1]	1.223(7)
C(2)–C(4)	1.32(2)
C(3)–C(4)[2]	1.38(3)
Fe(1)–O(2)	2.023(6)
F(1)–C(3)[1]	1.41(2)
O(2)–C(1)	1.223(7)
C(1)–C(2)	1.509(19)
C(2)–C(3)	1.33(2)
C(4)–C(3)[2]	1.38(3)
Fe(1)[3]–O(1)–Fe(1)	120.0
Fe(1)[3]–O(1)–Fe(1)[4]	120.0
Fe(1)–O(1)–Fe(1)[4]	120.0
C(1)–O(2)–Fe(1)	130.9(8)
O(2)–C(1)–O(2)[1]	128.6(13)
O(2)–C(1)–C(2)	115.6(7)
C(4)–C(2)–C(1)	121.4(12)
C(3)–C(2)–C(1)	124.9(13)

Symmetry transformations used to generate equivalent atoms: [1] $-x+y+1, y, z$ [2] $x-y, -y, -z$ [3] $-y+1, x-y, z$; [4] $-x+y+1, -x+1, -z+1/2$.

file has been deposited to Cambridge Crystallographic Data Centre (CCDC, http://www.ccdc.cam.ac.uk).

2.4. Thermogravimetric analysis

TGA was performed with TGA-S1000 (Scinco) under a constant flow of nitrogen gas. Approximately 10 mg of sample was loaded and the temperature was increased by 5 °C/min from 25 °C to 700 °C. Weight loss steps: 25–160 °C, −25.8% observed (−25.78% calculated for the loss of 3.5 DMF molecules); 250 °C, framework decomposition.

2.5. Gas sorption experiments

The adsorption isotherms of N_2 and H_2 at 77 K up to a pressure of 1 bar were measured using the standard volumetric procedure on a home-built instrument. Prior to measurement, the sample (∼100 mg) was outgassed at 50 °C under vacuum (10^{-3} Torr) for 6 h following overnight immersion in chloroform. The dead volume of the sample cell was measured three times using helium gas. Measured volumes of the analyte gases were delivered to the sample cell (cell volume = 27.29 mL) from a glass manifold that was evacuated and purged several times with the analyte gas before dosing. Pressure changes were monitored using ion pressure gauges and manually recorded after a typical equilibration time of 15 min. The temperature of the sample was maintained by immersing the sample cell in liquid nitrogen up to 1 cm above the material and the height of the coolant was kept at a constant level. To calculate the apparent Langmuir surface area, the nitrogen sorption data from the adsorption branch of the isotherm (range: $0 < P/P^0 < 0.9$) were fitted with the Langmuir equation and a molecular area of 16.2 $Å^2/N_2$ was assumed.

3. Results and discussions

3.1. Design and synthesis

Initial synthetic exploration with the perfluorinated link 2,3,5,6-tetrafluorobenzene-1,4-dicarboxylate was performed with the intention of preparing a functionalized analog of MOF-5 (also known as IRMOF-1, Zn_4O(benzene-1,4-dicarboxylate)$_3$) in order to investigate the influence of strongly electronegative groups on this material's hydrogen adsorption behavior. Previously it was observed that IRMOF-3 (Zn_4O(2-aminobenzene-1,4-dicarboxylate)$_3$) displays a slightly enhanced hydrogen uptake at low temperature and pressure [6,8]. Our modeling study indicated that the electron donating amino group may be responsible for this result, we attempted to make the analogous $Zn_4O(F_4BDC)_3$ to further investigate this electronic effect. Unfortunately, none of these syntheses were successful.

Moving instead to the iron system, we targetted a MOF isoreticular to MOF-235, which contains trigonal prismatic $Fe_3(\mu^3\text{-}O)(O_2C\text{–})_6$ clusters linked by benzene-1,4-dicarboxylate. Since the framework of MOF-235 has +1 charge per formula unit due to all iron having oxidation state +3, it is necessary for counter ions to reside in the pores, limiting the pore volume. To reduce the average oxidation state of the iron ions, we used $Fe^{II}Cl_2$ instead of $Fe^{III}Cl_3$ as the starting material. While solvothermal reactions typically produced amorphous or microcrystalline precipitates, we obtained well-formed single crystals when triethylamine vapor was slowly introduced into the reaction mixture at room temperature. The bulk phase purity of each sample was confirmed by comparison of the observed and simulated XRPD patterns (see Fig. 1).

3.2. Structural description

The X-ray structural analysis of **1** revealed the expected iron oxo clusters formed the inorganic SBUs. The central oxo atom lies on a special position (Wyckoff position *d* with site

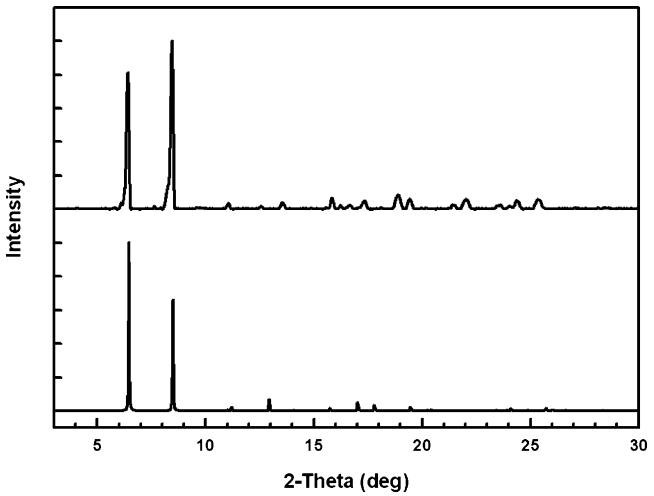

Fig. 1. XRPD patterns of the as-synthesized crystals (top) and the pattern calculated from the single crystal X-ray structure refinement (bottom).

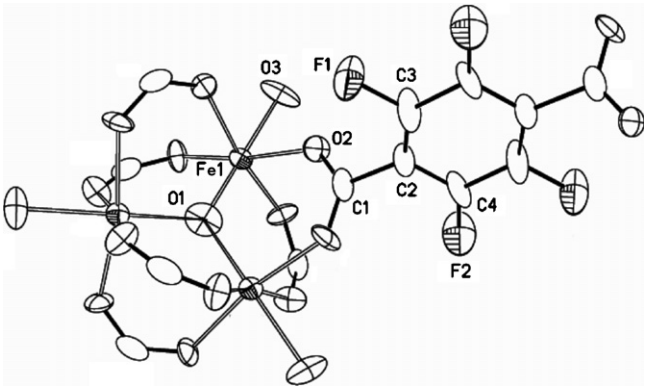

Fig. 2. Thermal ellipsoid plot of the inorganic secondary building unit and organic link in **1** with atomic numbering scheme. Atoms F1, F2, C3 and C4 of the organic moiety are disordered over two sites and only one conformation is shown here for clarity. O_3 is the oxygen atom of a coordinated water molecule. Ellipsoids are plotted at 50% probability, hydrogen atoms omitted for clarity.

symmetry of $-6m2$) with site occupancy factor 1/12. The crystallographically unique Fe ion lies on the Wyckoff position *h* with site symmetry of *mm*2. The asymmetric unit is composed of 1/12 of the $Fe_3O(F_4BDC)_3(H_2O)_3$ formula unit, if we consider the framework only. A thermal ellipsoid plot of the SBU and the F_4BDC link is represented in Fig. 2. The Fe ion has an octahedral coordination geometry composed of four carboxylate oxygen atoms, the oxo ion, and a terminal water molecule. Selected interatomic distances and angles are given in Table 2. The three equivalent Fe ions in the SBU are coplanar with an Fe···(μ_3-O)···Fe angle of 120°, as determined by the local symmetry, and the interatomic distance of Fe···Fe is 3.27 Å. The interatomic geometries are consistent with previously reported trivalent and mixed-valent $Fe_3O(O_2C–)_6$ clusters [16]. Based on the structural and elemental analyses, it is concluded that the oxidation states of the iron ions in **1** are mixed, with one Fe(II) and two Fe(III) ions per formula unit.

The inorganic SBU of **1** is very similar to that of MOF-235, $[Fe_3O(\text{benzene-1,4-dicarboxylate})_3(DMF)_3][FeCl_4]\cdot(DMF)_3$. In MOF-235 all of the iron have +3 oxidation state and DMF molecules are the terminal ligands on the cluster. Topological analysis determined that material **1** is also based on the *acs* net. A closer comparison of the two frameworks, however, reveals distinct conformational differences between the two links, as shown in Fig. 3. The torsion angle between the planes defined by the aromatic ring and the carboxylate moiety is 8° in the benzene-1,4-dicarboxylate (BDC) link of MOF-235 and 63° in the F_4BDC of **1**. This increased torsion angle stems from the larger size of the F atoms compared to H, and the partial negative charge of F that leads to unfavorable interactions with carboxylate oxygens. Ultimately this conformation change results in expansion of the channels in **1**, which run parallel to the crystallographic *c*-axis and have a 14.0 Å internal diameter, compared to 6.7 Å in MOF-235. The channels of **1** are surrounded by aromatic rings facing inward, reminiscent of carbon nanotubes, while in MOF-235 the edges of the

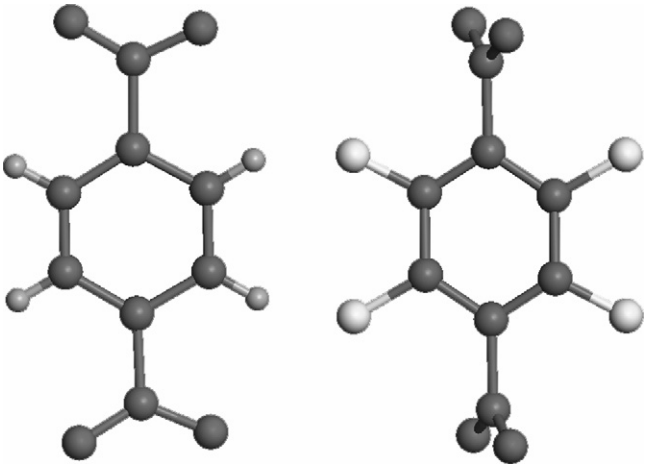

Fig. 3. Comparison of the conformations of the organic links in MOF-235 (BDC, left) and **1** (F_4BDC, right).

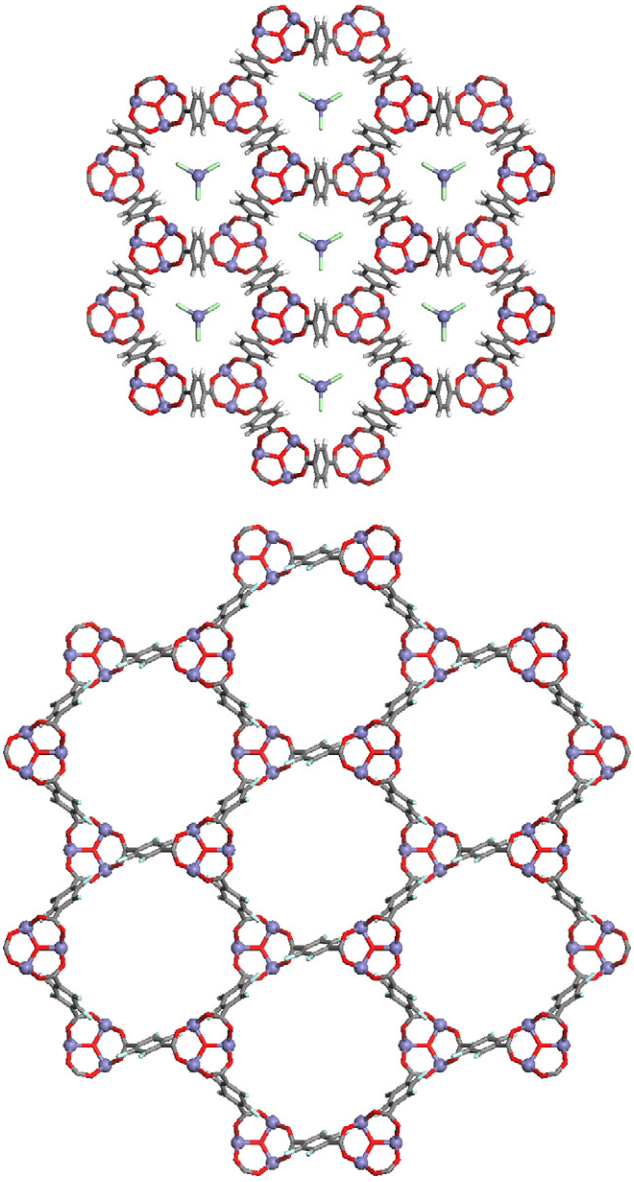

Fig. 4. Framework structures of MOF-235 (top) and **1** (bottom), viewed down the crystallographic *c*-axis. The guests in MOF-235 are $FeCl_4^-$ counter anions. Coordinated molecules and other guests in the channels have been omitted.

phenylene rings point inwards, reducing the internal diameter of the channels (see Fig. 4). Even if the $FeCl_4^-$ anions filling the channels of MOF-235 are ignored, the calculated pore volume of that material is less than 30%, whereas **1** has about 50% solvent accessible volume, as calculated by the program PLATON [17].

3.3. Porosity analysis

To remove the occluded DMF solvent molecules in the pores of **1** the filtered crystals were washed with chloroform three times and immersed in the solvent for 10 h. The sample was then filtered, quickly air-dried and loaded into the sample tube of the sorption apparatus. This activation procedure is typically performed to optimize the pore volume of MOF samples [6,10]. Nitrogen sorption data collected at 77 K demonstrated the microporosity of the sample by the reversible, hysteresis-free Type I isotherm (Fig. 5). Fitting of the adsorption branch of data resulted in a calculated apparent Langmuir surface area of 635 m^2/g. Hydrogen adsorption data were also collected at 77 K, revealing a portion of the expected Type I isotherm, however, saturation was not achieved at the highest pressure obtainable by the instrument. No hysteresis was observed, confirming the sorption process is physisorption. The amount of uptake at 1 bar was 0.9 wt%, which is comparable to other materials of this type.

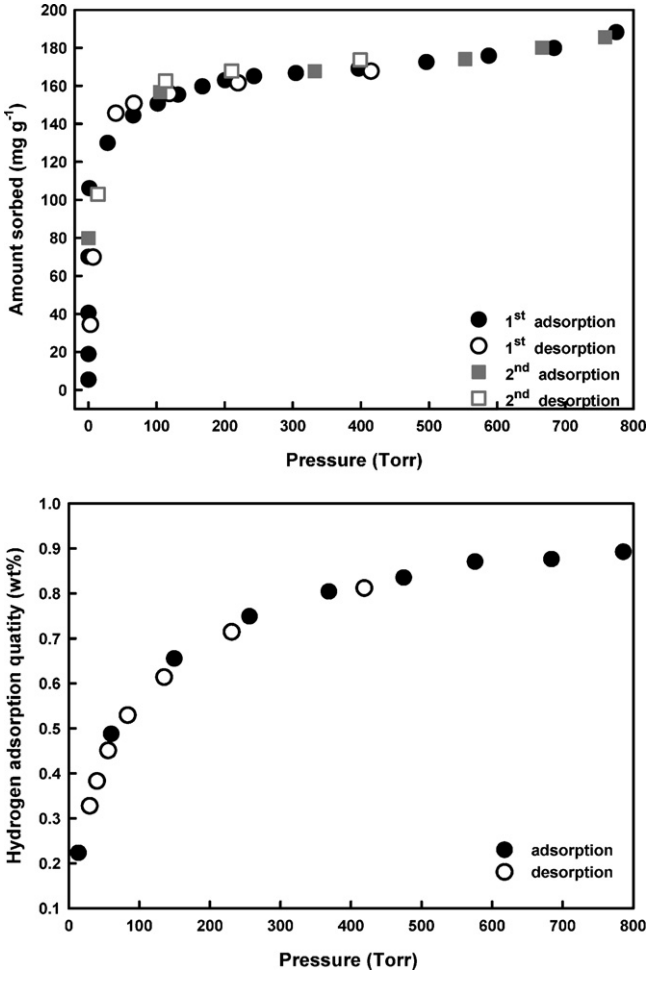

Fig. 5. Nitrogen (top) and hydrogen (bottom) sorption isotherms measured at 77 K.

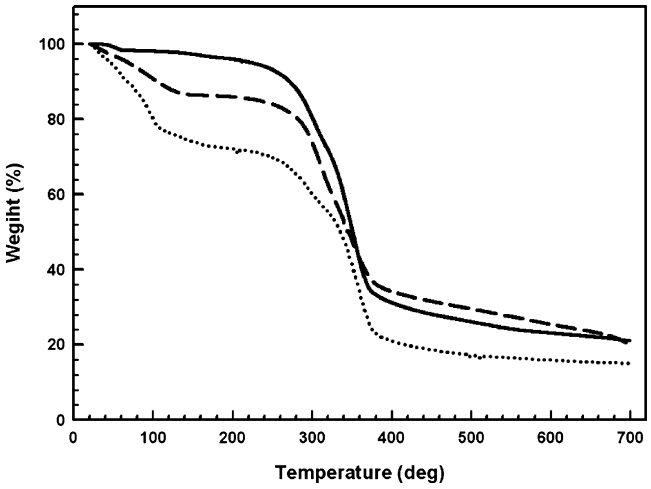

Fig. 6. TGA traces of **1** in the as-synthesized (dotted line), chloroform-exchanged (broken line), and fully outgassed states (solid line).

3.4. Thermogravimetric analyses and activation procedure

The as-synthesized material **1** lost 25.8% of its initial mass before 160 °C, corresponding to 3.5 DMF molecules per fomula unit occluded in the pore (Fig. 6). As the mass of the coordinated water molecules is just 5%, it is not clear whether they are also removed at this temperature. The bond distance between the water oxygen and the iron center, as determined crystallographically, is relatively long, suggesting that this bond is weak.

The reason for exchanging occluded DMF with the more volatile and non-coordinating chloroform is to reduce the thermal disruption to the framework during outgassing. When successful, this is evidenced in the TGA by a plateau showing the framework is empty and (presumably) stable before losing mass at the decomposition temperature. For the sample treated with chloroform, solvent loss was complete before 160 °C and the framework began to decompose at 250 °C. Based on these results, the outgassing temperature for the porosity studies was designated as 50 °C (under reduced pressure) to minimize thermal damage to the framework. After the sorption experiments, the TGA of the outgassed sample showed a single plateau extending to the decomposition temperature, confirming the completion of the outgassing procedure. The small mass loss at low temperature region is most likely to the desorption of atmospheric moisture that was adsorbed during the sample's brief exposure to air between the instruments.

4. Conclusions

We have successfully synthesized a porous mixed-valent iron MOF with the same inorganic secondary building unit and topology as previously reported non-porous MOFs with similarly sized organic links. The framework is neutral, with solvent-occluded channels 14.1 Å in diameter, significantly larger than MOFs of similar composition. The increased channel

size is due to the conformational change in the organic link imparted by functionalization with fluoro groups. The porosity of the material was demonstrated by hydrogen and nitrogen adsorption, making it one of the few iron-based MOFs with this property. Although the amount of hydrogen sorbed under our low temperature, low pressure conditions is small compared to other reported values, this work demonstrates how a minor conformational change – which is independent of topology – can yield a substantial increase in pore volume and hydrogen capacity.

Acknowledgements

This research was performed for the Hydrogen Energy R&D Center, one of the 21st Century Frontier R&D Programs funded by the Ministry of Science and Technology of Korea. We thank Accelrys Korea for the support of modeling software, and Dr. Jesse L.C. Rowsell for helpful suggestions during preparation of the article.

References

[1] Basic Research Needs for the Hydrogen Economy, United States Department of Energy, Report of the Basic Energy Sciences Workshop on Hydrogen Production, Storage, and Use, May 13–15, 2003, http://www.sc.doe.gov/bes/hydrogen.pdf.
[2] S. Franzky, Fuel Cells Bull. 9 (2002) 9.
[3] N.L. Rosi, J. Eckert, M. Eddaoudi, D.T. Vodak, J. Kim, M. O'Keeffe, O.M. Yaghi, Science 300 (2003) 1127.
[4] O.M. Yaghi, M. O'Keeffe, N. Ockwig, H.K. Chae, M. Eddaoudi, J. Kim, Nature 423 (2003) 705.
[5] S. Kitagawa, S.-I. Noro, Angew. Chem. Int. Ed. 43 (2004) 2334.
[6] J.L.C. Rowsell, O.M. Yaghi, J. Am. Chem. Soc. 128 (2006) 1304.
[7] J.L.C. Rowsell, O.M. Yaghi, Angew. Chem. Int. Ed. 44 (2004) 4670.
[8] D. Kim, T.B. Lee, S.B. Choi, J.H. Yoon, J. Kim, S.-H. Choi, Chem. Phys. Lett. 420 (2006) 256.
[9] N.W. Ockwig, O. Delgado-Friedrichs, M. O'Keeffe, O.M. Yaghi, Acc. Chem. Res. 38 (2005) 176.
[10] H. Li, M. Eddaoudi, M. O'Keeffe, O.M. Yaghi, Nature 402 (1999) 276.
[11] M. Eddaoudi, J. Kim, N. Rosi, D. Vodak, M. O'Keeffe, O.M. Yaghi, Science 295 (2002) 469.
[12] J.S. Seo, D. Whang, H. Lee, S.I. Jun, J. Oh, Y.J. Jeon, K. Kim, Nature 404 (2000) 982.
[13] K. Barthelet, D. Riou, G. Férey, Chem. Comm. (2002) 1492.
[14] G. Férey, C. Mellot-Draznieks, C. Serre, F. Millange, J. Dutour, S. Surblé, I. Margiolaki, Science 309 (2005) 2040.
[15] S. Surblé, C. Serre, C. Mellot-Draznieks, F. Millange, G. Férey, Chem. Comm. (2006) 284.
[16] A.C. Sudik, A.P. Cote, O.M. Yaghi, Inorg. Chem. 44 (2005) 2998.
[17] A.L. Spek, Platon, The University of Utrecht, Utrecht, The Netherlands, 1999.